08,10

Formation of the atomic and electronic structure of two-dimensional Si layers on $CrSi_2(0001)$

© N.I. Plyusnin[1], V.G. Zavodinsky[2], O.A. Gorkusha[2]

[1] Institute of Nanotechnologies of Microelectronics, Russian Academy of Sciences, Moscow, Russia
[2] Khabarovsk Branch of the Institute of Applied Mathematics, Far Eastern Branch of the Russian Academy of Sciences, Khabarovsk, Russia

E-mail: plusnin.n@inme-ras.ru

Received April 15, 2025
Revised May 26, 2025
Accepted May 27, 2025

A quantum mechanical simulation of the initial stage of Si growth at $CrSi_2(0001)$ has been performed. Growth was carried out by batch application of loose (0.3 ML portions) or dense (1 ML portions) Si atomic condensate to the surface of $CrSi_2(0001)$ frozen at 0 K, followed by its relaxation under the influence of quantum mechanical forces. It is shown that in the first case, Si surface phases are formed, consisting of an array of 2D and then 3D Si clusters with a tetrahedral sp^3 bond. And in the second case, the formation of a solid-phase wetting layer (TSS) Si occurs: first in the form of a pseudomorphic, and then a less stable polymorphic (packing) layer. The pseudomorphic solid-phase wetting layer, in this case, repeats the three-layer packing (ABC) of atoms in the $CrSi_2(0001)$ substrate, and the polymorphic solid-phase wetting layer, in addition to packing ABC, additionally acquires a two-layer packing of AB atoms. It has been found that, at least at 1−3 ML of Si, a density spectrum of electronic states characteristic of a metal is formed in a solid-phase Si wetting layer on $CrSi_2(0001)$.

Keywords: two-dimensional phases, solid-phase wetting layers, atom packing, phase transition, quantum mechanical modeling, Si, $CrSi_2(0001)$.

DOI: 10.61011/PSS.2025.05.61500.70-25

1. Introduction

At the initial stage of growth, coordination of atoms in a non-isostructural substrate $CrSi_2$ (parameter of hexagonal lattice $CrSi_2$ around: $a = 4.428$ Å and $c = 6.369$ Å) may impact coordination of atoms in the Si film (parameter of cubic lattice around: $a = 5.431$ Å). The study of this phenomenon is of interest from the point of view of thin film growth theory and technology development.

In the experiment the two-dimensional Si layers on $CrSi_2(0001)$, with solid phase growth, form amorphous or crystalline solid phase wetting layers (SPWL) of Si, which are adapted by density and structure to the substrate, have atomic density that is higher than that of bulk silicon, and are in metastable — stressed state under pressure pulled by the substrate [1–3]. In these Si SPWLs, as in silicon high pressure phases (for example, Si−II with Sn lattice [4]), you can expect metal conductivity. And since silicon has comparatively high value of spin coherence [5], these Si SPWLs may be potential candidates as new nanomaterials for spintronics.

Besides, single crystal $CrSi_2$ has application in microelectronic, optoelectronic, photovoltaic and thermoelectric devices and converters, since it is a narrow-bandgap semiconductor, compatible with technology of silicon microelectronics and having high temperature stability, thermoelectric capacity, electric conductivity and chemical resistance (see, for example, [6] — review in the introduction). One may expect that 2D Si on $CrSi_2$ film grown on Si substrate may also have application in appropriate instruments.

There are quite many papers on $CrSi_2$ epitaxy on a silicon substrate (see, for example [7–11]. But we found no papers on Si growth on $CrSi_2$ single crystal or epitaxial $CrSi_2$ films, except for papers [1,3]. As for the papers on modeling of Si SPWL growth on $CrSi_2$, none were found in the literature.

At the same time, in the previous articles, quantum-mechanical modeling demonstrated that the near coordination of atoms in metal SPWLs on silicon varies with their thickness, and this phenomenon causes phase transitions in SPWL and readjustment of the boundary layer of the substrate [12,13]. It is evident that in case of Si on $CrSi_2(0001)$ you should also expect changes caused by short-range order, since as in the case of metals on silicon, the volume phase of Si — is non-isostructural in respect to $CrSi_2(0001)$ substrate.

This article studied the quantum-mechanical modeling, which made it possible to research the change in the structure of surface phases and Si SPWLs on $CrSi_2(0001)$ depending on their density and thickness. This modeling demonstrated that Si SPWL, due to strong interaction with the substrate and proximity of atomic radii to it, acquires higher atomic density than in bulk silicon, besides, the

type of atomic packing in the substrate determines atomic packing in the film.

2. Research procedure

The film–substrate system state was modeled in steps — in statics. For this purpose, 2D Si condensate was applied in portions with thickness 1/3 ML and 1 ML (with low and, accordingly, high density) to the initial positions of the surface $CrSi_2(0001)$ (see below) under freezing conditions ($T = 0$ K). Then, every time, at each step, the system was relaxed — it changed to the minimum of free energy, moving with account of „benefit" (see below) of a certain structure [14]. Portions were applied in series: second — after relaxation of the first one etc.

Calculations were done using FHI96md [15] package working on the basis of the density functional theory [16,17], pseudopotential and plane wave collection methods. Pseudopotentials were generated using FHI98PP package [18]. One k-point of Brillouin zone was used for the collection of plane waves (0,0,0). The cutoff energy of the collection of plane waves was 40 Ry, and the exchange-correlation interaction was taken into account in the generalized gradient approximation [19].

Lattices of massive Si and $CrSi_2$ — are a volume-centered cubic one with the basis of two atoms for Si and hexagonal for $CrSi_2$. Close match of rows is available along faces (111) Si and (0001) $CrSi_2$. Besides, in lattice $CrSi_2$, in the direction parallel (0001) to the face, two schemes of dense atomic packing are combined (see Figure 1): ABC + AB (on options of dense packing of atoms in crystals — see, for example, [20]).

Figure 1 shows views on crystalline lattice $CrSi_2$ from the side of its four faces [21], and Figure 2 shows a hypothetical 2D Si lattice that is imposed upon 2D lattice of the upper layer $CrSi_2$ with rotation by 30° (on the left) and 0° (on the right). Besides, two atoms of its lattice cell are similarly inscribed into the lattice cell of layer $CrSi_2$, regardless of its orientation.

From Figure 1 you can see that $CrSi_2$ has hexagonal arrangement of six Si atoms around one Cr atom in the layers and packing of the top three layers — ABC. You can see that this hexagonal group of atoms is located coherently to the position of 7 atomic rows in $CrSi_2$ (black and grey balls). Besides, you can see that Si SPWL has a parameter of a 2D lattice, and its density is in 3/2 and, accordingly, 9/4 times higher vs the 2D layer of a Si(111) bulk phase — BP (brown balls).

To simplify the calculations, we limited ourselves to review of only the first three upper layers of the lattice $CrSi_2(0001)$ packed according to ABC scheme, since the next ones — deeper layers are screened by these layers and have weaker impact at Si packing.

Since atoms in Si SPWL on $CrSi_2(0001)$ follow the packing of upper (limited approximately by 3 lengths of screening) substrate atoms $CrSi_2$, i.e. „are adapted" to the

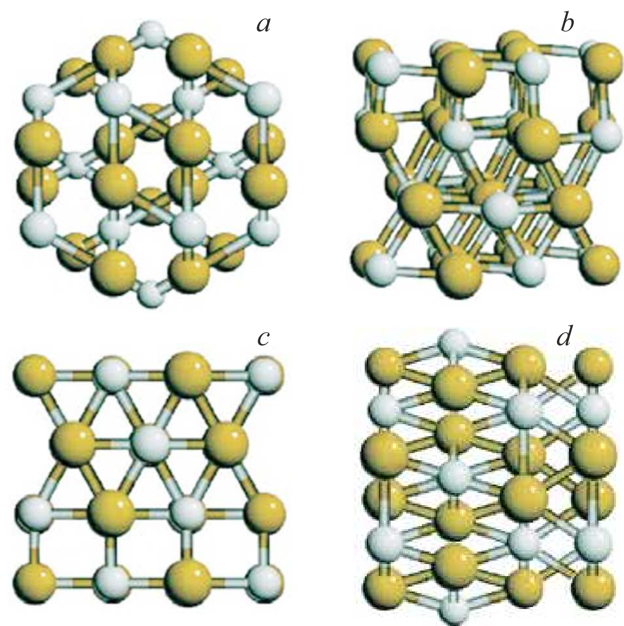

Figure 1. Views on different faces (a–d) lattices $CrSi_2$ [21]: a — face (0001). Si and Cr atoms — are brown and accordingly light-grey balls (the more atoms are pushed to the background, the smaller the atoms are).

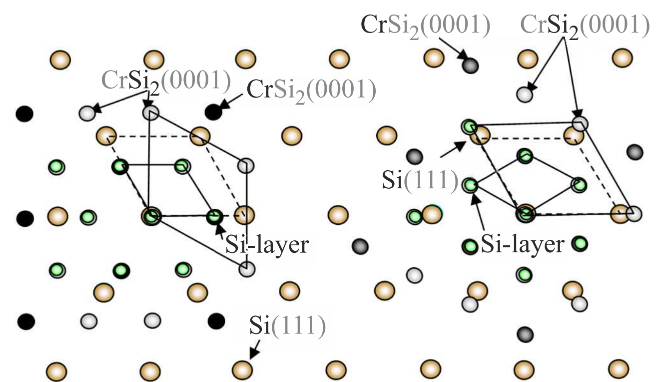

Figure 2. Hypothetical arrangement of atoms in a 2D layer of silicon, Si-layer (small balls), on top of atoms $CrSi_2(0001)$ (black balls — Cr and grey balls of medium size — Si), for the lattice $CrSi_2(0001)$, turned relative to Si(111) (large balls) on 30° (on the left) and 0° (on the right).

substrate, we suggested that in the first layers of SPWL the ABC packing is most probable, as in the substrate, even though in the subsequent Si SPWL layers a two-variant packing is possible: ABC or AB.

Limitation to only 3 upper layers $CrSi_2$ makes it possible to present the hexagonal lattice $CrSi_2$ in the form of a rectangular lattice with horizontal (in plane) dimensions: $a(X) = 9.875$ Å, $b(Y) = 6.899$ Å. Besides, vertical dimensions depend on its thickness or n — number of ML: $c(Z) = 5.73n$ Å.

Such rectangular supercell, after its transmission forms a superlattice multiple of $1\sqrt{3}$, i.e. $mn\sqrt{3}$. Transmission

of this rectangular supercell in the Cartesian coordinate system XY makes it possible to obtain an atomic system with substrate $CrSi_2$ in the form of a 2D sheet („slab").

Besides, we used, apart from a single-sided „slab" of Si on $CrSi_2(0001)$, a double-sided „slab" with Si growth — on the top and on the bottom. The double-sided „slab" made it possible to avoid the need for artificial fixation of lower layers $CrSi_2(0001)$. Besides, two sides of the „slab" reinforced the impact of surface layers $CrSi_2(0001)$ at Si growth.

When the single-sided „slab" was calculated, the supercell $CrSi_2$ was made of 6 ML $CrSi_2$. Besides, 3 lower ML supercells were artificially fixed, and 3 upper layers were relaxed (as well as the silicon layers applied on the top).

When the double-sided „slab" was calculated, the supercell $CrSi_2$ was made of two halves of 3 or 4 ML $CrSi_2$ each. Besides, its total length was, accordingly, $3 + 3 = 6$ ML or $4 + 4 = 8$ ML. Halves were made of hexagonal layers packed according to ABC scheme, as in the upper 3 layers $CrSi_2(0001)$ or, accordingly, — ABC + AB, as in the upper 4 layers $CrSi_2(0001)$.

The Si deposition method was as follows. We arranged the first layer-condensate centrally to the upper Cr atoms in $CrSi_2(0001)$, as shown in Figure 2 on the left. Such arrangement was selected based on the fact that the position of certain Si atoms on top of Cr atoms — is most beneficial from the energy point of view. We arranged the following monolayers using ABC, ABC + AB or AB schemes. Besides, after application of each subsequent layer, the atoms were relaxed to the minimum of the free energy in the system.

At each stage of the calculations, the energy growth was estimated (per single atom) using formula $\delta E_A = E_A/N_{Si} = (E - E_0)/N_{Si}$. Where E and E_0 — energy E_A of system $Si-CrSi_2$ at a certain stage and, accordingly, a certain „zero" reference point („reference" energy), and N_{Si} — number of Si atoms. Reduction in energy growth for a certain structure served as a parameter of its energy „benefit" and, in the next layer, this „beneficial" structure, together with a new layer, set the energy „benefit" of a new pack.

The built models, due to the small size of supercell $CrSi_2(0001)$, of course, did not allow accounting for the long-range order and superstructural coupling. Nevertheless, the calculation of the short-range order models made it possible to detect the common patterns in the change of the atom package in process of Si SPWL growth.

3. Findings and discussion

3.1. Superstructural coupling of 2D Si with $CrSi_2(0001)$

Figure 2 shows hypothetical ideal superstructural coupling of 2D lattices corresponding to dense monolayers of Si and $CrSi_2(0001)$. With the angle of 30° between them (on the left in the figure) or, accordingly, of 0° (on the right in the figure), these lattices are coupled at the ratios of $\sqrt{3/2}$ or 6/7. These ratios are close to the actual direct correspondence of 2D lattices (111) of non-dense Si BP and (0001) dense $CrSi_2$ BP — around 1.13 [8,11]. But the lattice cell of 2D lattice in a dense Si SPWL is less in the area than the cell of the non-dense Si BP 9/4 times.

If we extend the ideally coupled 2D Si and $CrSi_2(0001)$ lattices shown in Figure 2, and apply them onto each other, we will get the matching lattice points for both of the above angles, which will provide the superstructure $CrSi_2(0001)3\sqrt{3} \times 3\sqrt{3}-2DSi$. Besides, for angles between $CrSi_2(0001)$ and Si(111) 30° and 0° we will get the theoretical superstructures of angle match: $Si(111)2 \times 2-CrSi_2R30°$ and, accordingly, $Si(111)6/7 \times 6/7-CrSi_2R0°$.

These theoretical structures correspond to the low-energy electron diffraction (LEED) patterns obtained in papers [2,3]. We assume that $6/7 \times 6/7$ LEED pattern, in case of orientation R0°, was related to the periodicity of $CrSi_2(0001)$ as such induced by Si(111) substrate, and $3\sqrt{3} \times 3\sqrt{3}$ LEED pattern, in case of orientation R30°, — to the periodicity of the two-dimensional metastable Si SPWL as such on $CrSi_2(0001)$. Nevertheless, in case of orientation R0°, the $3\sqrt{3} \times 3\sqrt{3}$ LEED pattern was not observed. The possible reason for this — the fact that it was disturbed due to the stresses in the interface caused by lattice mismatch.

3.2. Growth of non-dense condensate

In most cases, as well as here, we used double-sided deposition of condensate on $CrSi_2(0001)$ substrate. Deposition was first carried out with increment 1/3 at./ML, and then — with increment 1/6 at./ML. Figure 3, *a–d* shows frontal (on the left) and side (on the right) views on $Si/CrSi_2(0001)/Si$ cell at Si thickness, accordingly: 2/3, 4/3, 5/3 and 11/6 ML.

The nature of structures in Figure 3 means that on $CrSi_2(0001)$, at thicknesses of 2/3 ML, 4/3 ML, 5/3 ML and 11/6 ML, 2D SP and layers. They consist: at 2/3 ML — of thinned atomic rows, at 4/3 ML and 5/3 ML — of 2D, and at 11/6 ML — of 3D clusters with tetrahedral sp^3 configuration of links (as in Si with the diamond lattice).

According to our calculations, Hartree energy (E_A) of two-dimensional system $Si/CrSi_2(0001)/Si$, at thicknesses 2/3 ML, 4/3 ML, 5/3 and 11/6 ML, is equal to, accordingly: −4.110, −4.000, −3.946 and −4.000 a.u.

Considering that the surface $CrSi_2(0001)$ has broken links and is not the most „beneficial", you can accept as the „reference" the lowest energy of the system −4.000 a.u. Accordingly, growth of energy (δE_A) relative to the „reference one", will amount to the above row of thicknesses in a.u. (v eV): −0.110 (2.99); 0 (0), 0.054 (1.47) and 0 (0). Therefore, the phase stability is increasing, decreasing and is increasing again. Besides, the stability is maximum in the first of these phases (at 2/3 ML). The subsequent growth of stability is explained by formation of tetrahedral sp^3 links.

In the following sections we will consider the growth of denser (adapted by density to $CrSi_2$) Si SPWL.

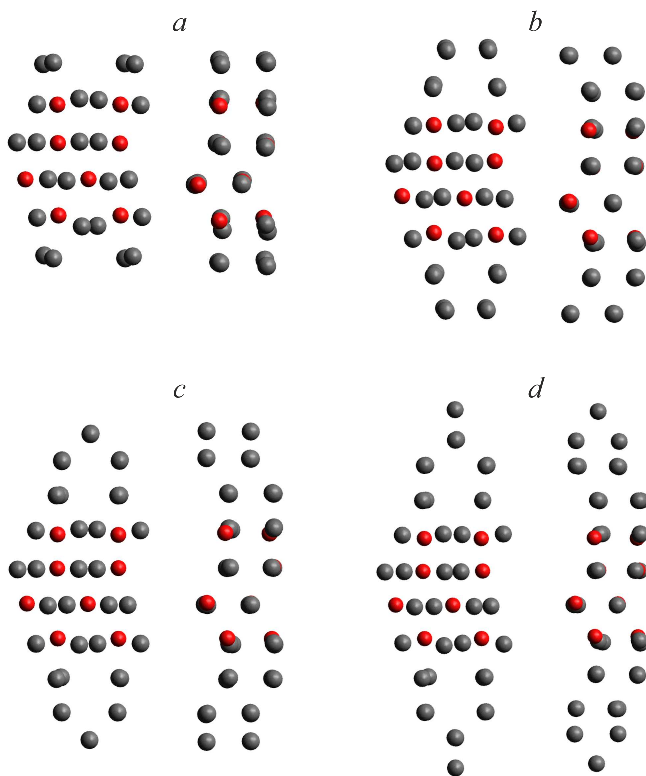

Figure 3. Frontal and side view of Si/4 ML $CrSi_2(0001)$/Si at Si thickness: *a* — 2/3 ML, *b* — 4/3 ML, *c* — 5/3 ML, *d* — 11/6 ML.

3.3. Growth of non-dense condensate

Figure 4, *a–c* and Figure 4, *e* show the frontal (on the left) and side (on the right) views on $Si/CrSi_2(0001)$, at thickness $CrSi_2$ 3 ML and thickness of Si condensate (prior to its relaxation), accordingly: 0 ML, 1 ML, 3 ML and 7 ML. And Figure 4, *d* shows the top view onto upper two layers of $Si/CrSi_2(0001)$ structure. Where the light brown and black balls are — the first (upper) and, accordingly, the underlying second Si layers. Note that in the following sections we will not show on the figures the upper and side projections, since further the packing of rows in these projects has not changed practically.

Figure 4, *d* shows packing of two upper Si layers. The side view in Figure 4, *a–c* and Figure 4, *e* on the right shows that atoms in Si SPWL, regardless of its thickness, form rows with the same packing of rows as in the substrate. The frontal view in Figure 4, *a–c* and Figure 4, *e* on the left also shows that, at Si thickness 1–2 ML, in the rows as such the packing repeats the ABC packing of the substrate. At Si thickness 3–7 ML, the packing is arranged according to AB scheme (except for the first two layers and, accordingly, of the 1st layer), which is also confirmed by Figure 4, *d*.

In general it means that the mixed packing is formed: in the first 1–3 layers — ABC packing, and in the subsequent ones — AB. Besides, the more is the film thickness, the largest share of the thickness is occupied by AB packing. Therefore, at 7 ML, only the 1st layer is exposed to the substrate, and the entire Si SPWL is weakly stabilized by the substrate (at 7 ML. this happens possibly because the thickness of SPWL is more than the substrate thickness).

Figure 5 shows densities of electron states $CrSi_2(0001)$ and unilateral heterostructures $Si/CrSi_2(0001)$ with Si thickness 1 ML and 3 ML.

You can see from these averaged curves that the drop at the Fermi level on the spectrum of substrate $CrSi_2(0001)$ decreases considerably after deposition of already the 1st ML Si. Besides, the level of density of states near the Fermi level and in the entire spectrum at 1–3 ML Si increases considerably, and at 3 ML Si it even spreads beyond its limits (7.5–10 eV).

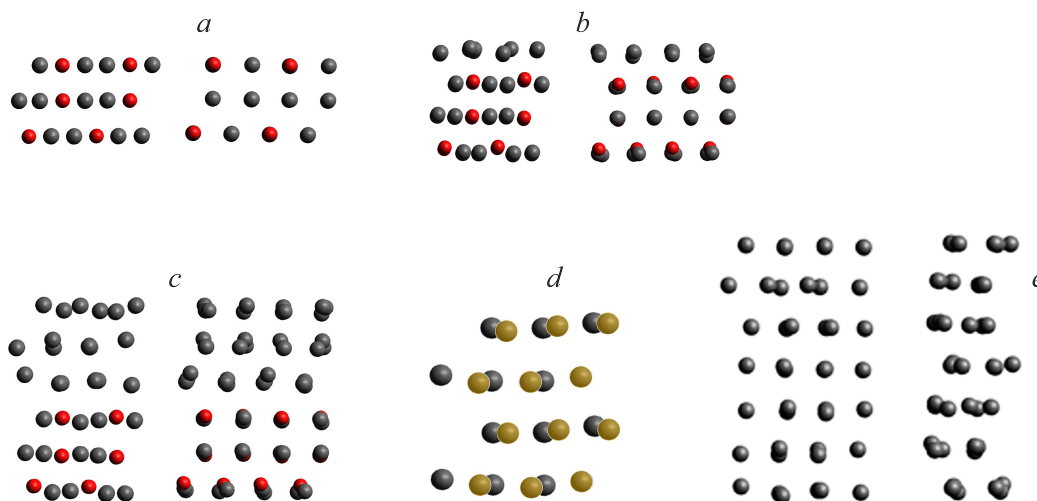

Figure 4. Frontal (on the left) and side (on the right) views (*a–c* and *e*) and top view (*d*) on Si/3 ML $CrSi_2(0001)$ at Si thickness: 0 ML (*a*), 1 ML (*b*), 3 ML (*c,d*) and 7 ML (*e*). Where (*a*) — supercell prior to relaxation, and light-brown balls on (*d*) — upper layer of Si.

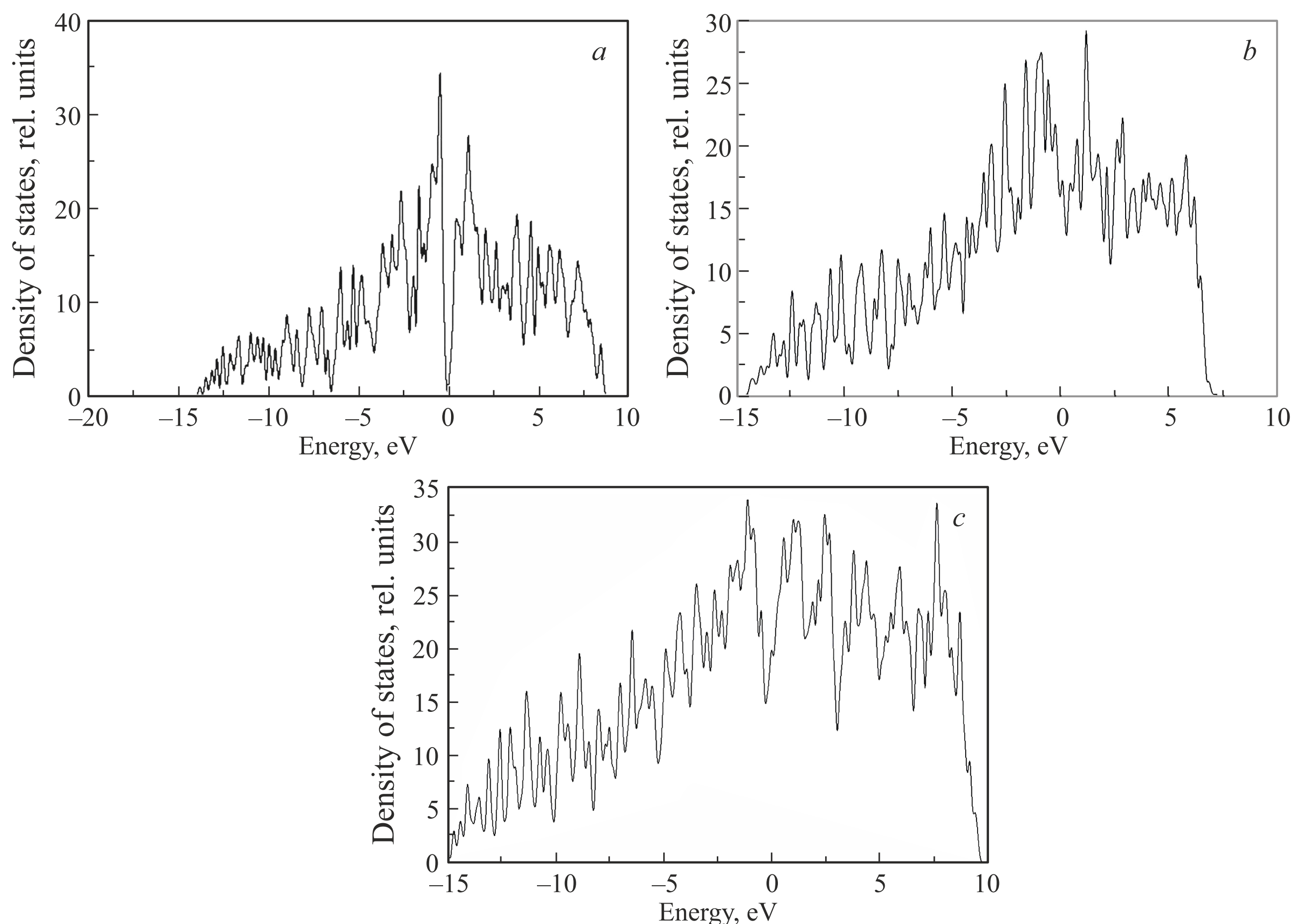

Figure 5. Density of electron states in substrate $CrSi_2$ (a) and in heterostructures $Si/CrSi_2(0001)$ (see Figure 4) with Si thickness 1 ML (b) and 3 ML (c).

Therefore, if we subtract the density of states of the substrate, we will get the disappearance of the band gap and appearance of the density of metal states, both near the Fermi level (at 1 ML), and beyond (at 3 ML). This is indicated by formation of a two-dimensional Si SPWL on $CrSi_2(0001)$ at 1 ML, and a certain two-dimensional/pseudo-bulk metal Si SPWL at 3 ML.

Under two-sided growth of Si in supercell $CrSi_2(0001)$, which was produced by joining two halves with thickness of 3 ML (see Figure 6), a more pronounced deformation of $CrSi_2$ substrate took place. We assume this happens due to imbalance of the electron density on the surface $CrSi_2$ and in its volume. However, at 1 ML Si, this deformation disappears, evidently, due to the return of the balance of electron density, and at 3 ML it reappears.

It is interesting that in Figure 6,f ABC packing extends to 4 ML. Therefore, symmetrical cross-linking of 2 halves increases the SPWL thickness with ABC packing. This means that the impact of substrate layers that are deeper than 3 ML may not still be completely excluded.

Nevertheless, as you can see from Figure 7 and comparison with Figure 6, ABC packing at thickness of substrate $CrSi_2(0001)$ 8 ML, changes to AB packing after 3 ML Si. The fact that ABC packing in Figure 7 is stable to 3 ML, may be explained by screening of substrate effect, since three dense monolayer of Si are close in thickness to 3 lengths of Fermi screening in metal.

Therefore, as Si SPWL grows on $CrSi_2(0001)$, first a certain „screening“ Si layer is growing. Besides, up to 3 ML the ABC packing is preferable, and complete substrate screening is not yet available. Further the packing type changes from ABC to AB and at thicker thickness the AB packing becomes more beneficial.

3.4. Competition of packings in supercells of various thickness

Table 1 contains calculations for $CrSi_2$ with thickness 6 ML. The least value of energy, for ABC and AB packings, in all tables is indicated with bolt font. From Table 1 you can see that the system energy and its growth, in case of ABC packing, reaches „deep“ minimum at 2 ML and SPWL with ABC scheme becomes more stable. Further, at 3–5 ML, SPWL with AB packing scheme becomes more metastable and beneficial. However, the stability of this SPWL to „critical“ thickness of 4 ML somewhat decreases,

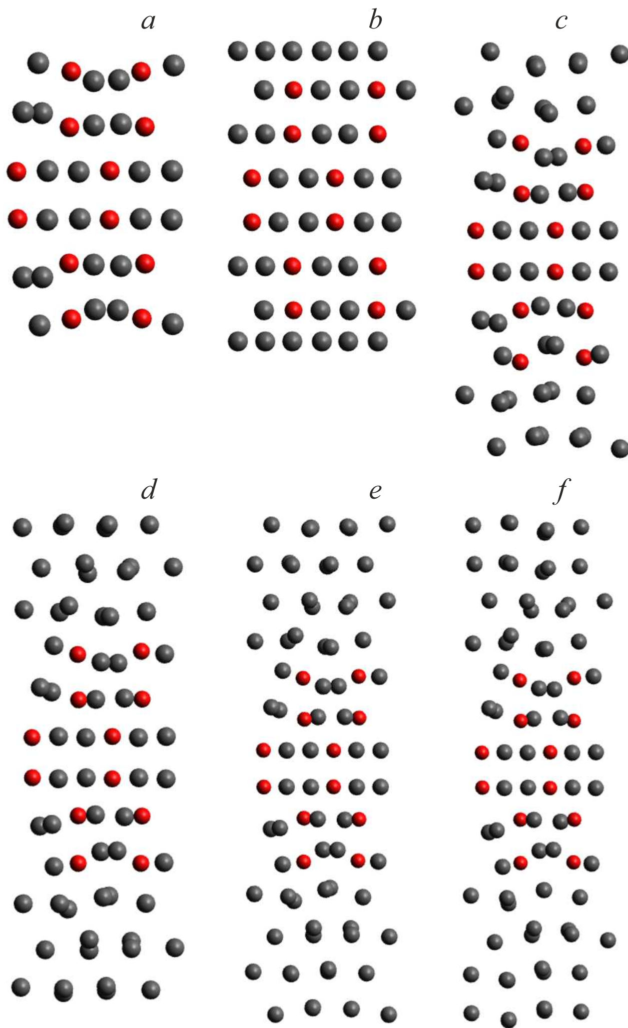

Figure 6. Frontal view on Si/6 ML $CrSi_2$(0001)/Si with Si thickness: *a* — 0 ML, *b* — 1 ML, *c* — 2 ML, *d* — 3 ML, *e* — 4 ML, *f* — 5 ML.

and then, at 5 ML, both packings become beneficial at the same time. This means that SPWL after „critical" thickness becomes polymorphous.

Most probably, at 3 ML, the ABC packing of the substrate is screened, and it becomes less beneficial. Besides, the SPWL tendency to form a hexagonal AB type packing reaches maximum. However, the stability of this SPWL and AB type packing further drops with the thickness due to the decrease in the stabilizing impact of the substrate, and ABC packing remains nearly constant. Therefore, at 5 ML the probability of two packings becomes equally probable. As we assume, under further deposition this competition will change with origination of Si BP and transition of Si SPWL to Si BP.

Table 2 contains calculations for $CrSi_2$ supercell with thickness 8 ML. Comparison with Table 1 shows that the new $CrSi_2$ supercell increases energy and energy growth in the system, which indicates the decrease of its stability. Besides, at $CrSi_2$ supercell thickness of 8 ML and Si thickness of 1−2 ML, the degree of stability of ABC and AB packings is „levelled". However, in general the system behavior remains the same.

Most probably, the reduction in the stability of the system and the above „leveling" are related to even (four) quantity of layers in the halves of the supercell, which disturbs the „ideality" of ABC packing at the boundary of these two halves. At the same time you must consider that

Table 1. Energy per atom (E_A) and its growth (δE_A) in respect to $E_A = -4.0000$ for structure Si/$CrSi_2$(0001)-6ML/Si at different Si thicknesses and atom packings: the bold font identifies the most beneficial packing for each thickness

Thickness	Packing scheme			
	ABC		AB	
	E_A, a.u.	δE_A, a.u. (eV)	E_A, a.u.	ΔE_A, a.u. (eV)
1	**−3.9864**	**0.0136 (0.37)**	−3.8682	0.1318 (3.58)
2	**−3.9896**	**0.0104 (0.28)**	−3.9840	0.016 (0.44)
3	−3.9835	0.0165 (0.45)	**−3.9846**	**0.0154 (0.42)**
4	−3.9829	0.0171 (0.47)	**−3.9838**	**0.0162 (0.44)**
5	**−3.9839**	**0.0161 (0.44)**	**−3.9839**	**0.0161 (0.44)**

Table 2. Energy per atom (E_A) and its growth (δE_A) in respect to $E_A = -4.0000$ for structure Si/$CrSi_2$(0001)-8ML/Si at different Si thicknesses and atom packings: the bold font identifies the most beneficial packing for each thickness

Thickness	Packing scheme			
	ABC (Figure 6)		AB	
	E_A, a.u.	δE_A, a.u. (eV)	E_A, a.u.	ΔE_A, a.u. (eV)
1	**−3.9820**	**0.018 (0.49)**	−3.9740	0.026 (0.71)
2	**−3.9830**	**0.017 (0.46)**	−3.9810	0.019 (0.52)
3	−3.9814	0.0186 (0.51)	**−3.9828**	**0.0172 (0.47)**
4	−3.9796	0.0204 (0.55)	–	–

Table 3. Energy per atom (E_A) and its growth (δE_A) in respect to $E_A = -4.0000$ for structure Si-ABC/$CrSi_2$ (0001)-8ML/Si-ABC of various thickness, with the arrangement of a Si monolayer with AB packing on top of it

Si thickness, ML		ABC+AB structure	
Sublayer, ABC packing	Top-layer, AB packing	E_A, a.u.	δE_A, a.u. (eV)
2	1	**−3.9837**	**0.0163 (0.44)**
3	1	−3.9814	0.0186 (0.51)

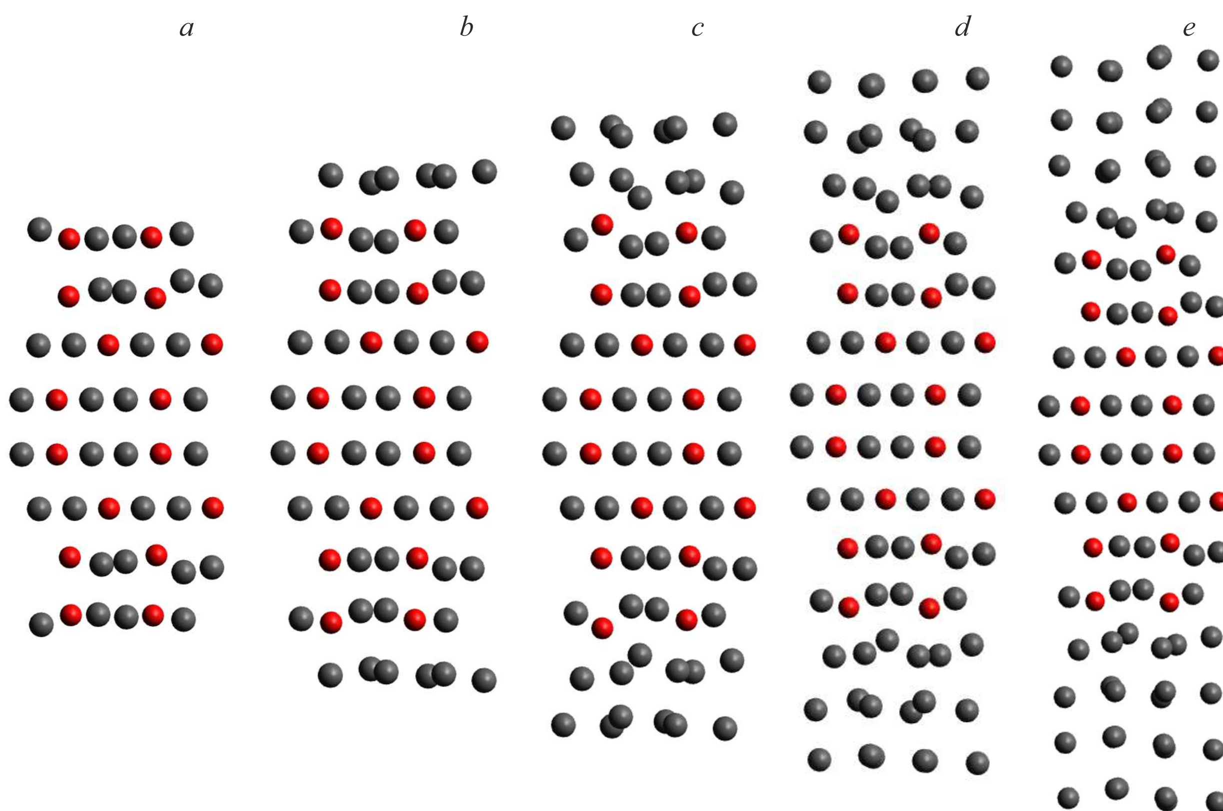

Figure 7. Frontal view at $Si/CrSi_2(0001)/Si$ structure at thicknesses $CrSi_2$ 8 ML and Si: *a* — 0 ML, *b* — 1 ML, *c* — 2 ML, *d* — 3 ML, *e* — 4 ML.

such disturbance of „ideality" in the 4th layer also occurs in the real lattice $CrSi_2(0001)$ (see Figure 1). Therefore, growth at supercell thickness $CrSi_2$ 8 ML, better reflects „the second side of the medal" at SPWL growth — packing polymorphism.

Table 3 provides the energy values at Si monolayer arrangement with AB packing at both sides of structure Si-ABC/$CrSi_2(0001)$/Si-ABC.

Comparison to Table 2 shows that at 3 ML the mixed ABC packing (2 ML) + AB (1 ML) is more stable than AB packing (3 ML). Therefore, prior to formation of Si volume phase, it is possible to change to a thicker polymorphous SPWL, containing, apart from ABC packing, AB packing of hexagonal type. Nevertheless, in all cases the maximum stability of Si SPWL is achieved with the ABC packing scheme at 2 ML Si, which corresponds to the experiment [2,3].

4. Conclusion

Quantum-mechanical modeling of Si growth was carried out on plates $CrSi_2(0001)$ in the form of supercell $Si/CrSi_2(0001)$ or $Si/CrSi_2(0001)/Si$ transmitted along the plane. When non-dense Si condensates are modeled, formation of 2D surface phases and two-dimensional array of 3D Si clusters with tetrahedral sp^3 configuration of interatomic links was found. When dense Si condensates were modelled, it was shown that Si SPWL was growing with electronic structure of two-dimensional metal, and this two-dimensional metal at 1−2 ML is growing with the packing according to ABC scheme, and after 2−3 ML, — with packing according to AB scheme with further transition to polymorphous ABC + AB packing.

Conflict of interest

The authors declare that they have no conflict of interest.

References

[1] N.I. Plyusnin. Condens. Matter Interphases **25**, *4*, 594 (2023). https://doi.org/10.17308/kcmf.2023.25/11471
[2] N.I. Plusnin, N.G. Galkin, V.G. Lifshits, A.P. Milenin. Phys. Low-Dim. Struct. (PLDS) **1–2**, 55 (1999). https://elibrary.ru/item.asp?id=13307399
[3] N.I. Plyusnin, N.G. Galkin, V.G. Lifshits, A.P. Milenin. Poverkhnost. Rentgenovskie, sinkhrotronnye i nejtronnye issledovaniya, **16**, *6*, 22 (2000). (in Russian). http://www.issp.ac.ru/journal/surface/2000/06-2000.htm/ N.I. Plusnin, N.G. Galkin,
[4] S.M. Jeong, T. Kitamura. Jpn. J. Appl. Phys. **46**, *9R*, 5924 (2007). https://doi.org/10.1143/jjap.46.5924

[5] F.A. Zwanenburg, A.S. Dzurak, A. Morello, M.Y. Simmons, L.C. Hollenberg, G. Klimeck, S. Rogge S.N. Coppersmith, M.A. Eriksson. Rev. Mod. Phys. **85**, *3*, 961 (2013). https://doi.org/10.1103/revmodphys.85.961
[6] S.O. Mathias, Y. Malozovsky, L. Franklin, D. Bagayoko. J. Mod. Phys. **9**, *14*, 2457 (2018). https://doi.org/10.4236/jmp.2018.914158
[7] V.G. Lifshits, V.G. Zavodinsky, N.I. Plyusnin. Poverkhnost. Fizika, khimiya i mekhanika **3**, 82 (1983). (in Russian).
[8] F.Y. Shiau, H.C. Cheng, L.J. Chen. J. Appl. Phys. **59**, *8*, 2784 (1986). https://doi.org/10.1063/1.336990
[9] A. Rocher, A. Oustry, D.M. Josée, M. Caumont. J. Vac. Sci. Technol. A: Vac. Surf. Films **12**, *6*, 3018 (1994). https://doi.org/10.1116/1.578930
[10] N.I. Plusnin, N.G. Galkin, V.G. Lifshits, S.A. Lobachev. Surf. Rev. Lett. **2**, *4*, 439 (1995). https://doi.org/10.1142/s0218625x9500039x
[11] O. Filonenko, A. Mogilatenko, H. Hortenbach, F. Allenstein, G. Beddies, H.J. Hinneberg. J. Cryst. Growth **262**, *1–4*, 281 (2004). https://doi.org/10.1016/j.jcrysgro.2003.10.054
[12] V.G. Zavodinsky, N.I. Plyusnin, O.A. Gorkusha. ZhTF **94**, *2*, 231 (2024). (in Russian). https://doi.org/10.61011/JTF.2024.02.57077. 199-23
[13] N.I. Plyusnin, V.G. Zavodinsky, O.A. Gorkusha. FTT **66**, *2*, 275 (2024). (in Russian). https://doi.org/10.61011/FTT.2024.02.57251.273
[14] X. Gonze, B. Amadon, P.-M. Anglade, J.-M. Beuken, F. Bottin, P. Boulanger, F. Bruneval, D. Caliste, R. Caracas, M. Côté, T. Deutsch, L. Genovese, Ph. Ghosez, M. Giantomassi, S. Goedecker, D.R. Hamann, P. Hermet, F. Jollet, G. Jomard, S. Leroux, J.W. Zwanziger. Comput. Phys. Commun. **180**, *12*, 2582 (2009). https://doi.org/10.1016/j.cpc.2009.07.007
[15] M. Bockstedte, A. Kley, J. Neugebauer, M. Scheffler. Comput. Phys. Commun. **107**, *1–3*, 187 (1997). https://doi.org/10.1016/S0010-4655(97)00117-3
[16] P. Hohenberg, W. Kohn. Phys. Rev. **136**, *3B*, B864 (1964). https://doi.org/10.1103/PhysRev.136.B864
[17] W. Kohn, L.J. Sham. Phys. Rev. **140**, *4A*, A1133 (1965). https://doi.org/10.1103/PhysRev.140.A1133.
[18] M. Fuchs, M. Scheffler. Comp. Phys. Commun. **119**, *1*, 67 (1999). http://dx.doi.org/10.1016/S0010-4655(98)00201-X.
[19] J.P. Perdew, W. Yue. Phys. Rev. B **33**, *12*, 8800 (1986). https://doi.org/10.1103/PhysRevB.33.8800
[20] N.V. Belov. Struktura ionnykh kristallov i metallicheskikh faz, Izdatelstvo Akademii Nauk SSSR, M. (1947). (in Russian). https://ufn.ru/ru/articles/1947/9/m/
[21] Crystal Lattice Structures: (21 Oct 2004): The $CrSi_2$ (C40) Structure. online resource — https://www.atomic-scale-physics.de/lattice/struk/c40.html

Translated by M.Verenikina